Study of Phase-Noise Properties and Timing Jitter of 40-GHz All-Optical Clock Recovery Using Self-Pulsating Semiconductor Lasers

Jeremie Renaudier, Bruno Lavigne, Philippe Gallion, *Senior Member, IEEE,* and Guang-Hua Duan, *Senior Member, IEEE*

***Abstract*—This paper reports on timing-jitter analysis of an all-optical clock-recovery scheme at 40 GHz using self-pulsating (SP) lasers. Based on the analogy with injection locking of oscillators, theoretical investigations on phase-noise properties of the recovered clock lead to the demonstration of a filtering function with slope that is compliant with the International Telecommunications Union (ITU) standards and allow us to underline the dependence of the cutoff frequency of the filtering transfer function on the spectral linewidth of the free running SP laser. From this phase-noise analysis, an analytical expression of the timing jitter of the recovered clock is derived, including the optical signal-to-noise ratio (OSNR) of the injected signal. A set of experiments on all-optical clock recovery at 40 GHz is then presented and demonstrates the crucial role of the spectral linewidth on the timing-jitter-filtering function of the SP laser. In good agreement with theoretical results, the impact of the OSNR degradation of the injected signal on the timing jitter is also demonstrated. Finally, the all-optical clock-recovery operation using a quantum-dot SP laser is shown to be standard compliant in terms of timing jitter, even for highly degraded OSNR.**

***Index Terms*—Clock recovery, injection-locked oscillators, semiconductor lasers.**

I. Introduction

DUE TO ceaseless growth of Internet traffic, the development of practical means for all-optical signal processing, such as all-optical digital logic functions or retiming, reshaping, and reamplifying (3-R) regenerators, is attracting great interest in order to improve transmission distance, transparency, and speed of optical networks [1], [2]. Thus, all-optical regeneration at 40 Gb/s and beyond appears to be a crucial element for future transparent networks. One solution to achieve the regeneration is the combination of a Mach–Zehnder interferometer with an all-optical clock-recovery element [2], [3]. Among the different approaches investigated so far to accomplish the clock-recovery function, a scheme based on the optical injection locking of a single self-pulsating (SP) semiconductor laser is of particular interest from practical and cost viewpoints [4].

The aim of a clock-recovery scheme is twofold: to recover the clock pulses from the bit rate of an incoming data signal and to filter the noncorrelated timing jitter from this signal. The first point has already been investigated experimentally in an extensive manner with different types of SP semiconductor lasers. Several configurations of SP distributed-feedback (DFB) lasers like phase-comb [4], [5], active-mirror [6], and gain-coupled [7]–[9] DFB have successfully demonstrated the possibility to lock the free running SP frequency to the clock frequency of an incoming data signal. This potential has also been reported using SP distributed Bragg resonator (DBR)-type lasers, either with [10] or without saturable absorber [11]. All these components, based on bulk or quantum-well structures, have shown promising results at high bit rates in terms of frequency tuning range, insensitivity to wavelength, and polarization state of the incoming signal. However, little information has been given on the jitter characteristics of the recovered clocks. Nevertheless, it is very important to compare the jitter-filtering functions of SP lasers with ITU-T standards for clock-recovery schemes.

To address the issue of timing-jitter filtering expected from all-optical clock-recovery schemes, we propose a theoretical analysis of phase-noise properties of injection-locked SP lasers. From a phenomenological approach proposed in [12], based on an analogy with Adler's work [13] describing the phase noise of injection-locked microwave oscillators, an analytical expression of the phase-noise power spectral density (PSD) of injection-locked SP lasers is used to describe the timing-jitter-filtering phenomenon. Then, the importance of the free running spectral linewidth ($\Delta\nu$) of SP lasers is pointed out to achieve more efficient high-frequency jitter-filtering functions because this parameter determines the cutoff frequency of the injection-locked SP laser. The impact on timing jitter of optical signal-to-noise-ratio (OSNR) degradation of the injected signal is also investigated. To illustrate these theoretical remarks, the experimental comparison between the phase-noise properties of two SP lasers, having largely different $\Delta\nu$, is reported. An excellent agreement is found between measurements and calculation results, demonstrating the importance of $\Delta\nu$ on the jitter transfer function cutoff frequency of an injection-locked SP laser. Finally, all-optical clock-recovery experiments at 40 Gb/s are presented to demonstrate the impact of this parameter and of amplified spontaneous emission (ASE) noise on the timing-jitter characteristics of the recovered clock.

Manuscript received April 6, 2006; revised June 28, 2006.

J. Renaudier is with Alcatel—Thales III–V Laboratory, 91767 Palaiseau, France, and also with ENST Paris, LTCI UMR 5141, 75634 Paris, France (e-mail: jeremie.renaudier@3-5lab.fr).

B. Lavigne is with Alcatel Research and Innovation, 91460 Marcoussis, France (e-mail: bruno.lavigne@alcatel.fr).

P. Gallion is with ENST Paris, CNRS LTCI UMR 5141, 75634 Paris, France (e-mail: philippe.gallion.enst.fr).

G.-H. Duan is with Alcatel—Thales III–V Laboratory, 91767 Palaiseau, France (e-mail: guanghua.duan@3-5lab.fr).

Digital Object Identifier 10.1109/JLT.2006.882432

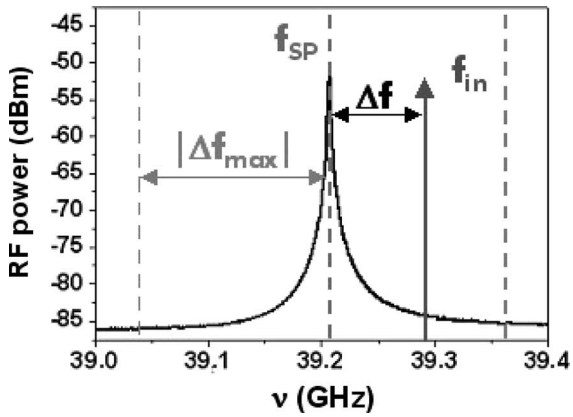

Fig. 1. Schematical description of the involved parameters in injection-locking phenomena.

II. Theoretical Analysis of Phase Noise and Timing Jitter of the Recovered Clock

Exhaustive study of timing jitter of an RF oscillator requires a theoretical analysis of the PSD of the phase noise around the carrier frequency. Focusing on the clock-recovery application, our analysis deals with the phase noise of an SP laser synchronized by an external optical clock, which means that the influence of the data pattern delivered by the input signal was not taken into account in the numerical analyses. In this respect, f represents in the following the analysis frequency defined as the frequency offset around the studied carrier frequency.

A. Phase-Noise Properties of the Recovered Clock

The main elements to develop this analysis are the characteristic parameters of both the free running SP laser and the injected optical-clock signal. On the one hand, those of the SP laser are its free running SP frequency $f_{\rm SP}$ and its intrinsic phase-noise PSD $S_{\phi_{\rm SP}}$. By analogy with laser oscillators where the electric field has a Lorentzian shape around the optical frequency [14], [15], the Lorentzian shape of the radio frequency (RF) spectrum observed experimentally [16] leads by inverse Fourier transform to the following expression of $S_{\phi_{\rm SP}}$ [12]:

$$S_{\phi_{\rm SP}}(f) = \frac{\Delta\nu}{2\pi f^2}. \tag{1}$$

On the other hand, the injected optical clock is characterized by its own frequency $f_{\rm in}$ and its phase-noise PSD $S_{\phi_{\rm in}}$. Since the frequency of this clock can differ from the SP frequency, we define this frequency shift as Δf. Of course, the injection-locking regime of the SP laser will be highly dependent on this frequency shift, so that we can define a locking bandwidth $\Delta f_{\rm max}$ as the maximum value of frequency shift below which the laser keeps locked. All these parameters are schematically illustrated by Fig. 1. It is to be noted here that the locking bandwidth developed in [12] depends on the laser structure and on the input-signal characteristics, such as power and wavelength separation. In particular, it has been shown [12] that the locking bandwidth is proportional to $\Delta\nu$ and to the power ratio defined as the ratio between the output power of the SP-laser signal and the injected optical power of the input signal. Thus, for a given power ratio, the locking bandwidth $\Delta f_{\rm max}$ is all the more short as the spectral linewidth $\Delta\nu$ is small. In other words, the higher the spectral purity of the SP laser is, the shorter the maximum tolerable frequency shift will be. This result is similar to that derived from the properties of the well-known Adler's equation [13] that describes the synchronization in phase of microwave oscillators. One can however underline here a difference between these two approaches: The term of injection ratio involves the optical power, and not the electric field, in the case of the SP laser.

From the parameters defined above, the phenomenological approach developed by Duan and Pham [12], by analogy with Adler's works, leads to the following expression of the phase-noise PSD S_{ϕ_L} for injection-locked SP lasers:

$$S_{\phi_L}(f) = \frac{f_L^2}{f^2+f_L^2}\cdot S_{\phi_{\rm in}}(f) + \frac{f^2}{f^2+f_L^2}\cdot S_{\phi_{\rm SP}}(f) \tag{2}$$

in which f_L represents the locking characteristic frequency of the injection-locking phenomenon. This key parameter is defined by the following expression [12]:

$$f_L = \sqrt{\Delta f_{\rm max}^2 - \Delta f^2}. \tag{3}$$

Since the locking characteristic frequency is the square root of the difference between the square of the locking bandwidth and that of the frequency shift, one can note that the largest value for this parameter is obtained for a zero frequency shift between the free running SP laser and the injected optical clock.

The phase-noise PSD expressed by (2) enables us to point out the existence of three distinct operating regimes mainly determined by the locking characteristic frequency depicted in Fig. 3.

1) $f \ll f_L$: The phase noise of the injection-locked laser is dominated by the one of the injected optical clock. In other words, the injected clock conveys its phase-noise properties to the recovered clock. Hence, this regime corresponds to a transparency region with respect to the injected clock signal.
2) $f \gg f_L$: The contribution of the free running SP laser to the phase noise of the injection-locked laser prevails, so that the latter is no more affected by the phase-noise properties of the injected clock signal.
3) $f \sim f_L$: The region in the vicinity of f_L is likely to be a transition regime where the contributions of both the free running SP laser and the injected clock are mixed.

Considering a Lorentzian phase-noise PSD (1) for the free running SP laser, the expression of the phase-noise PSD of the injection-locked laser expressed by (2) can be rewritten as follows:

$$S_{\phi_L}(f) = \frac{1}{1+\left(\frac{f}{f_L}\right)^2}\cdot\left(S_{\phi_{\rm in}}(f) + \frac{\Delta\nu}{2\pi f_L^2}\right). \tag{4}$$

This expression of the phase noise of the injection-locked laser reveals the appearance of a second-order filtering function with a -3-dB cutoff frequency being the locking characteristic frequency f_L. Moreover, the second member of the last term,

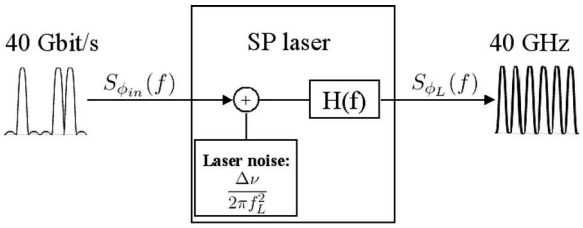

Fig. 2. Schematical representation of the SP laser as an active filtering element.

representing the phase-noise contribution of the free running SP laser, shows that the SP laser has to be considered as an active filtering element rather than a passive one, as it is schematically described in Fig. 2. One can note that the SP-laser-noise contribution is fully described by $\Delta\nu$ and the square of the locking characteristic frequency f_L. It is important to remark that these two parameters are not actually independent. f_L is related to $\Delta\nu$ via the locking-bandwidth term $\Delta f_{\max}$. Hence, the phase-noise contribution of the free running SP laser is mainly determined by $\Delta\nu$. This point may be underlined by introducing the linewidth to cutoff frequency ratio $\rho = \Delta\nu/f_L$ into expression (4) of the phase-noise PSD of the injection-locked laser, leading to the following equation:

$$S_{\phi_L}(f) = H(f) \cdot \left(S_{\phi_{\text{in}}}(f) + \frac{\rho^2}{2\pi\Delta\nu} \right) \tag{5}$$

where we have introduced the phase-noise transfer function of the injection-locked SP laser $H(f)$ defined by

$$H(f) = \frac{1}{1 + \left(\frac{f}{f_L}\right)^2}. \tag{6}$$

This transfer function represents a second-order low pass filter with a 20-dB/dec decrease compliant with ITU-T recommendations. As for electronic filtering elements, the key parameter that governs the efficiency of such a low-pass filter is the -3-dB cutoff frequency, determined here by the locking characteristic frequency f_L. For the sake of simplicity, we can consider in the following a zero frequency shift $(\Delta f = 0)$ between the SP laser and the injected optical clock. In this case, the locking characteristic frequency becomes equal to the locking bandwidth of the studied SP laser. As previously explained in this section, the locking bandwidth of the SP laser depends not only on $\Delta\nu$ but also on the power ratio. Because the injected power of the input signal is an external parameter of the SP laser, it cannot be used to control f_L. Hence, $\Delta\nu$ is the only key parameter that must be used to optimize the performances of the all-optical-clock-recovery scheme. This idea is schematically represented on Fig. 3 for a fixed power ratio and a given laser structure, e.g., for which ρ is fixed. The evolution of the phase noise of the injection-locked laser (solid curves) is established from the phase noises of the injected signal (long-dashed curve) and the SP laser (short-dashed curves) for two different values of $\Delta\nu$ such as $\Delta\nu_1 > \Delta\nu_2$. It is to be noticed that the phase noises of the SP laser are still described under the Lorentzian approximation. This schematic description illustrates that a narrower $\Delta\nu$ leads to a smaller

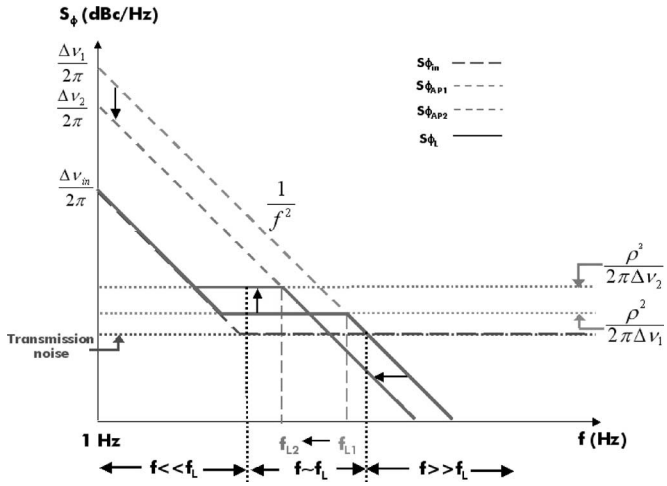

Fig. 3. Schematical representation of the impact of the free running spectral linewidth on the cutoff frequency for a given laser structure.

cutoff frequency but also to a larger additional noise in the transition region. To summarize, in order to improve the all-optical-clock-recovery performances, we have pointed out the important role of $\Delta\nu$ because it determines the cutoff frequency of the second-order filtering function.

B. Timing Jitter of an SP-Laser-Based Clock Recovery

By definition, the rms timing jitter of any clock signal is determined by its phase-noise PSD according to the following relation:

$$\sigma = \frac{1}{2\pi f_0} \cdot \sqrt{\int_{-\infty}^{+\infty} S_{\phi_L}(f) df} \tag{7}$$

with f_0 being the frequency of the considered clock. From the expression of the phase-noise PSD of the injection-locked laser given by (2), the timing jitter of the recovered clock can be split into two distinct contributions

$$\sigma = \sqrt{\sigma_{\text{in}}^2 + \sigma_{\text{SP}}^2} \tag{8}$$

with

$$\sigma_{\text{in}} = \frac{1}{2\pi f_{\text{in}}} \cdot \sqrt{\int_{-\infty}^{+\infty} \frac{f_L^2}{f^2 + f_L^2} S_{\phi_{\text{in}}}(f) df}$$

$$\sigma_{\text{SP}} = \frac{1}{2\pi f_{\text{in}}} \cdot \sqrt{\int_{-\infty}^{+\infty} \frac{f^2}{f^2 + f_L^2} S_{\phi_{\text{SP}}}(f) df}. \tag{9}$$

The calculation of the contribution of the SP laser to the overall timing jitter can be developed under the Lorentzian approximation for the free running SP-laser phase noise and is expressed by

$$\sigma_{\text{SP}} = \frac{1}{2\sqrt{2}\pi f_{\text{in}}} \cdot \sqrt{\rho}. \tag{10}$$

According to (10), Fig. 4 gives the evolution of the timing jitter induced by the free-running SP laser as a function of ρ for a clock frequency f_{in} fixed at 40 GHz. One may observe

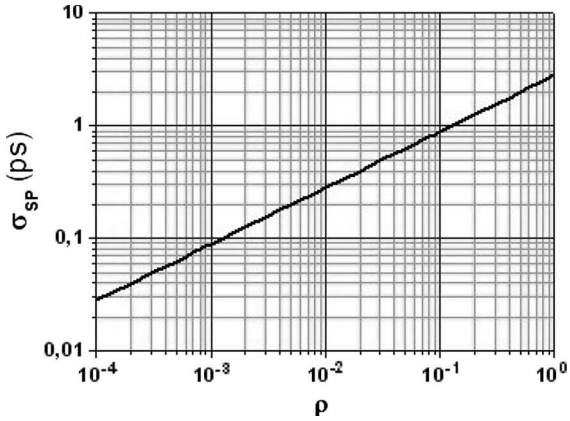

Fig. 4. Evolution of the timing jitter introduced by the free running SP laser.

qualitatively on this figure that ρ must be lower than 10^{-2} to make the timing-jitter contribution of the SP laser lower than 300 fs.

C. Influence of the OSNR of the Incoming Signal

The influence of the OSNR of the incoming signal on the timing jitter of the recovered clock can be obtained by analyzing the beating between ASE noise and the clock component, as well as the ASE–ASE beating. According to calculations detailed in the Appendix, the phase-noise PSD of the incoming signal may be written as follows:

$$S_{\phi_{\rm in}}(f) = S_{\phi_{\rm ck}}(f) + \frac{1}{B_0 m^2} \times \left[\frac{2}{\rm OSNR} + \left(1 - \frac{f_{\rm in}+f}{B_0}\right)\left(\frac{1}{\rm OSNR}\right)^2\right] \quad (11)$$

where $S_{\phi_{\rm ck}}$ is the phase-noise PSD of the single optical clock, m is the modulation depth of the optical clock defined as the ratio between the peak power and the average power, B_0 is the bandwidth of the filter placed in front of the SP laser, and OSNR is the OSNR inside B_0. From this expression, the timing jitter of the recovered clock brought by the incoming signal can be split into two distinct contributions

$$\sigma_{\rm in} = \sqrt{\sigma_{\rm ck}^2 + \sigma_{\rm OSNR}^2} \quad (12)$$

with the clock contribution $\sigma_{\rm ck}$ and the ASE noise contribution $\sigma_{\rm OSNR}$ being expressed by (13), shown at the bottom of the page.

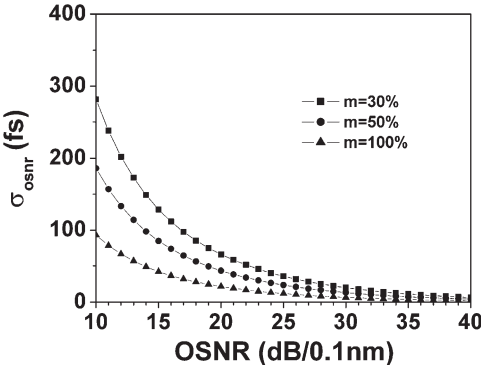

Fig. 5. Evolution of the timing jitter introduced by the OSNR degradation of the incoming signal.

Taking into account that the cutoff frequency f_L is largely smaller than the carrier frequency $f_{\rm in}$, the calculation of the jitter contribution due to ASE noise leads to the following expression of $\sigma_{\rm OSNR}$:

$$\sigma_{\rm OSNR} = \frac{1}{2\sqrt{2}\pi f_{\rm in}} \cdot \sqrt{\frac{2\pi f_L}{B_0 m^2}\left[\frac{2}{\rm OSNR} + \left(1 - \frac{f_{\rm in}}{B_0}\right)\left(\frac{1}{\rm OSNR}\right)^2\right]}. \quad (14)$$

According to (14), Fig. 5 gives the evolution of $\sigma_{\rm OSNR}$ with respect to OSNR of the incoming signal for a clock frequency $f_{\rm in}$ fixed at 40 GHz and for different modulation depth. One may see that the OSNR impact on the recovered-clock timing jitter is almost negligible for values greater than 30 dB/0.1 nm. As expected, the impact of ASE noise is growing up when the modulation depth is decreasing.

In conclusion, the total timing jitter of the recovered clock can be expressed as follows:

$$\sigma = \sqrt{\sigma_{\rm ck}^2 + \sigma_{\rm SP}^2 + \sigma_{\rm OSNR}^2} \quad (15)$$

where $\sigma_{\rm ck}$, $\sigma_{\rm SP}$, and $\sigma_{\rm OSNR}$ correspond to the input-signal contribution, the intrinsic SP-laser noise, and the incoming ASE noise contribution, respectively.

III. Experimental Part: Comparison With Theory and All-Optical-Clock-Recovery Evaluation

A. Experimental Setup and SP-Laser Description

We display in Fig. 6 the experimental setup used to test SP lasers at 40 Gb/s. The amount of jitter of the incoming data signal is adjusted by triggering the pattern generator with a

$$\sigma_{\rm ck} = \frac{1}{2\pi f_{\rm in}} \cdot \sqrt{\int_{-\infty}^{+\infty} \frac{f_L^2}{f^2 + f_L^2} S_{\phi_{\rm ck}}(f) df}$$

$$\sigma_{\rm OSNR} = \frac{1}{2\pi f_{\rm in}} \cdot \sqrt{\int_{-\infty}^{+\infty} \frac{f_L^2}{f^2 + f_L^2} \frac{1}{B_0 m^2}\left[\frac{2}{\rm OSNR} + \left(1 - \frac{f_{\rm in}+f}{B_0}\right)\left(\frac{1}{\rm OSNR}\right)^2\right] df} \quad (13)$$

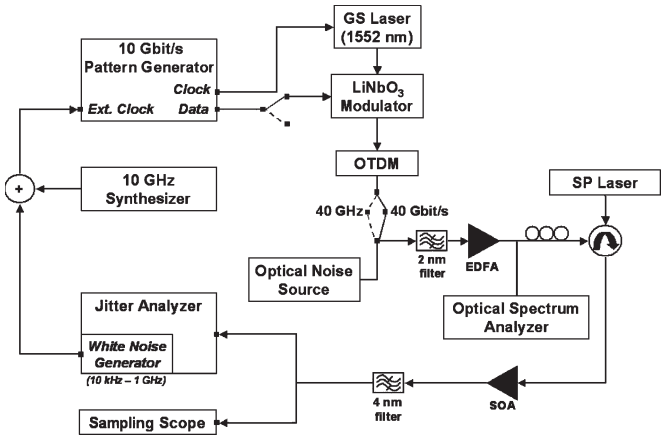

Fig. 6. Experimental setup for phase-noise characterization of SP-laser-based all-optical-clock recovery at 40 GHz.

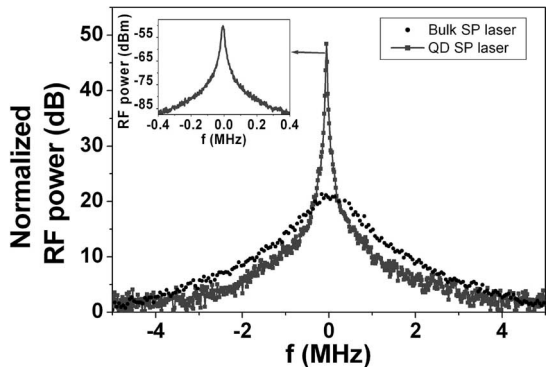

Fig. 7. Comparison of the RF spectra obtained in the case of bulk DBR laser (straight line) and of QD laser (dotted line).

10-GHz external clock provided by a synthesizer, the jitter of which is monitored by a white-noise generator (10 kHz–1 GHz) provided by the Europtest jitter analyzer. Thus, the pattern generator provides both a 10-GHz clock signal and a $2^{31}-1$ pseudorandom binary sequence (PRBS) at 10 Gb/s that drive, respectively, a gain-switched laser (lasing at 1552 nm), and a $LiNbO_3$ modulator. The so-obtained 10-Gb/s RZ signal is then launched into the OTDM system that delivers the 40-Gb/s RZ signal. We recall that such a multiplexer does not provide pure PRBS signal for sequences longer than 2^7-1 because of the very large required delay between 10-Gb/s tributaries. When no PRBS data drive the external modulator, the OTDM signal delivers a 40-GHz optical clock that will be considered later on as the reference clock. This configuration will be used in the next section in order to compare theoretical results with experimental ones. The OTDM signal is then injected into the SP lasers through a circulator, and the recovered-clock signal is amplified and filtered by a 4-nm bandwidth optical filter before being analyzed either on the sampling scope or by the jitter analyzer. The Europtest jitter analyzer provides phase-noise spectra from which we can extract the rms jitter in the bandwidth 100 Hz–500 MHz. In addition, we have added an optical noise source that will be amplified along with the signal by the clock preamplifier.

The SP semiconductor lasers under study are both made of a buried ridge structure. The first one is a DBR laser containing a bulk active layer. The second one is a single-section Fabry–Pérot (FP) laser containing a quantum-dot (QD) active layer on InP substrate(100) (see [17] for more details). It is worth noticing that SP originates in both lasers from passive mode locking [18], [19]. The cavity structure difference (DBR or FP) affects only the number of longitudinal modes and does not have any impact on the clock-recovery performance. Table I summarizes the main features of each laser along with their respective operation conditions.

Fig. 7 shows the beating spectra of both lasers in the free running regime measured by means of a high-speed photodiode followed by an electrical spectrum analyzer (ESA), with a resolution bandwidth set to 3 kHz. $\Delta\nu$ is measured to be 1 MHz for the bulk DBR laser and 20 kHz for the QD laser (see inset of Fig. 7), respectively. The very small value of $\Delta\nu$ of the QD laser is believed to be the consequence of a strong laser modes correlation due to favorable four-wave-mixing in QD structures. In the following experiment, an optical-clock signal is injected into each laser with a frequency equal to their own SP frequency.

B. Phase-Noise Characteristics: Theory and Experiment

Fig. 8 depicts phase-noise measurements performed on both SP lasers along with the phase-noise spectrum of the reference clock. The noise floor of the jitter analyzer is also reported in this figure. As described in Section II-A, three distinct regions can be observed. For frequencies lower than 60 kHz, the phase noise from the injected clock signal dominates, corresponding to the so-called transparent region. One can also easily observe the filtering region far from the carrier frequency, with a 20-dB/dec decrease of the phase noise. Between these two regions, the transition region can be distinguished, in which the noise is dominated by the contribution of the free running SP laser. These phase-noise curves also allow us to point out clearly the shorter cutoff frequency obtained with the QD laser, leading to a better filtering effect than with the bulk laser. Consequently, this experimental observation demonstrates that a decrease of $\Delta\nu$ leads to a decrease of the cutoff frequency of the jitter-filtering function, as may be expected from the theoretical predictions of Section II. Moreover, one can note in Fig. 8 that the phase-noise level of the QD laser decreases down to the apparatus noise floor.

In order to verify the theoretical-model predictions, we have interpolated the experimental results with the phase-noise expression from (4) using $\Delta\nu$ and f_L as fitting parameters. In addition, the measured phase noise of the reference clock is used as $S_{\phi_{\text{in}}}$. As may be seen in Fig. 9, we obtain a very good agreement between the theoretical model and the experimental results for both lasers. The parameters used for interpolation were $\Delta\nu$ values of 1 MHz and 10 kHz and f_L values of 60 MHz and 5.5 MHz, respectively, for the bulk and the QD lasers. The 1-MHz $\Delta\nu$ of the bulk laser obtained from interpolation is also equal to that measured on the ESA, confirming the validity of the theoretical model. The difference observed in the case of the QD laser between $\Delta\nu$ values extracted from ESA spectrum and interpolation originates from the test-bench instabilities during measurements of $\Delta\nu$ on an ESA. Indeed, such instabilities

TABLE I
CHARACTERISTICS OF THE LASERS UNDER STUDY

	Bulk DBR laser	QD FP laser	Units
Length	1120	1050	μm
Central lasing wavelength	1520	1500	nm
Operating conditions	280	230	mA
Self-pulsation frequency (f_{SP})	40.28	40.28	GHz
Free running spectral linewidth ($\Delta\nu$)	1000	20	kHz

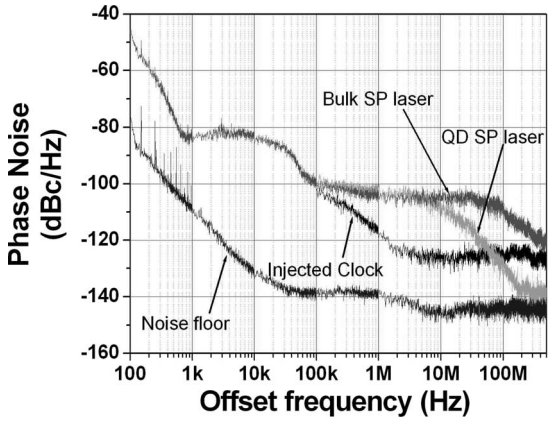

Fig. 8. Phase-noise spectra of the reference clock, the recovered clock from the bulk SP laser, and that from the QD SP laser. The lower spectrum indicates the noise floor of the apparatus.

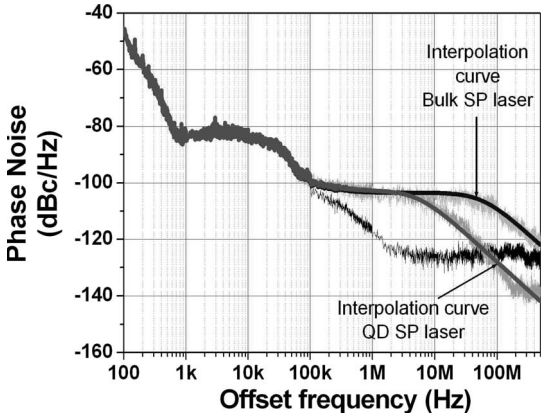

Fig. 9. Fitting curves of phase-noise spectra of the recovered clocks from the bulk SP laser and the QD SP laser.

reduce measurement accuracy for spectral linewidths of the order of some kilohertz. From $\Delta\nu$ and f_L values, we deduce from (10) intrinsic jitters of 350 and 100 fs for the bulk and QD lasers, respectively.

The very short cutoff frequency of 5.5 MHz for the QD laser is very close to the value expected from the ITU-T G825.1 recommendations for clock-recovery schemes at 40 GHz. To confirm this observation, we calculated the jitter transfer function $H(f)$ of the SP lasers from (6) considering the f_L values extracted from interpolation. The calculated transfer functions of the bulk SP laser and the QD SP laser are represented in Fig. 10, as well as the transfer function defined by the ITU-T G825.1

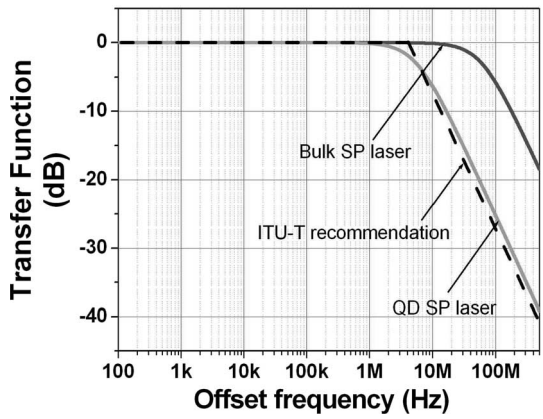

Fig. 10. Phase-noise transfer function of the Bulk SP laser and the QD SP laser compared to ITU recommendation.

recommendations for clock-recovery schemes at 40 GHz. We clearly conclude in this figure the good matching of the QD-laser transfer function with ITU-T recommendation template, as demonstrated in [20].

C. All-Optical-Clock-Recovery Evaluation

This section is devoted to the characterization of all-optical-clock recoveries when injecting 40-Gb/s RZ data coded by PRBS of $2^{31}-1$. In that case, the input signal contains data components alongside the clock frequency that will be transferred to the recovered clock within the locking range. Such data to clock transfer is compliant with ITU-T standards because it does not have any impact on the clock-recovery performance [20]. Experimentally, we have verified that the recovered data components are at least 20 dB lower than the recovered-clock component. Therefore, the evaluation of the all-optical-clock-recovery performance will be carried out by considering only the impact of the input jitter and the ASE noise.

1) Impact of Input Jitter: The shorter cutoff frequency exhibited by the QD SP laser implies a better jitter-filtering function compared to the bulk SP laser. To get more insight into this behavior, we have experimented the evolution of the timing jitter of the recovered clocks delivered by both lasers as a function of the input jitter of the incoming data signal. The jitter degradation of the injected optical clock is monitored through the jitter analyzer, which generates a white noise in the frequency range 10 kHz–1 GHz with a variable level. For each amount of added noise, we determined the jitter carried by the

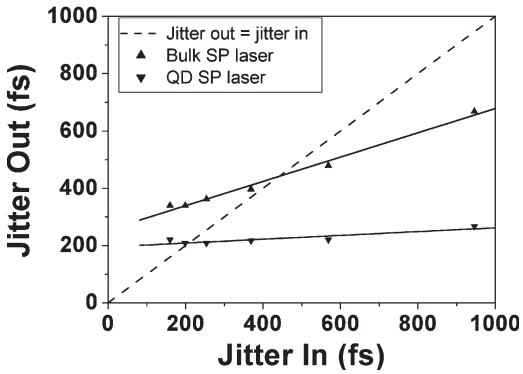

Fig. 11. Evolution of the jitter of the recovered clocks versus the jitter of the incoming signal for the Bulk SP laser and the QD SP laser.

input signal and the recovered clocks in the frequency range 100 Hz–500 MHz. Fig. 11 shows the evolution of the timing jitters of the recovered clocks delivered by both SP lasers versus the input jitter. We have also reported in this figure a dashed line of slope 1 representing the function for which the output jitter is equal to the input jitter. We observe for both lasers a nearly linear evolution of the output jitter with respect to the input jitter, with a larger slope for the bulk laser because of larger $\Delta\nu$. Besides, when comparing both curves, we observe the better jitter-filtering effect of the QD laser. Therefore, these measurements demonstrate the key role played by $\Delta\nu$ in the performance of the all-optical-clock recovery.

2) Impact of Degraded OSNR: To complete the experimental study of SP laser, the impact of the OSNR degradation on the quality of the recovered clock has been studied using the QD laser only. As previously described (see Fig. 6), optical noise is added to the 40-Gb/s signal by means of an optical fiber amplifier (electrical spectrum analyzer) and amplified along with the signal by an in-line fiber amplifier. The resulting OSNR of the incoming data signal is measured on an optical ESA. A 2-nm-bandwidth (B_0) optical filter is placed in front of the SP lasers to reduce the out-of-band noise. Fig. 12(a) shows an example of the eye diagram of the incoming signal with a degraded OSNR of 21 dB/0.1 nm. The recovered clock delivered by the QD SP laser from this incoming signal is depicted in Fig. 12(b), showing an extinction ratio greater than 13 dB and low timing jitter. The complete results of the evolution of the recovered-clock timing jitter (in the frequency range 100 Hz–500 MHz) as a function of the OSNR of the incoming data signal are given by Fig. 13. The dashed curve represents the interpolation function of experimental data deduced from the theoretical evolution of the timing jitter given by (14). This curve is obtained by considering the impact of OSNR degradation that is negligible for values higher than 30 dB/0.1 nm, so that one can write

$$\sigma_1 = \sqrt{\sigma_{\mathrm{ck}}^2 + \sigma_{\mathrm{SP}}^2} \approx 187 \text{ fs}. \tag{16}$$

In this way, the theoretical impact of OSNR degradation expressed by (14) can be added to obtain the overall timing jitter of the recovered clock as follows:

$$\sigma = \sqrt{\sigma_1^2 + \sigma_{\mathrm{OSNR}}^2}. \tag{17}$$

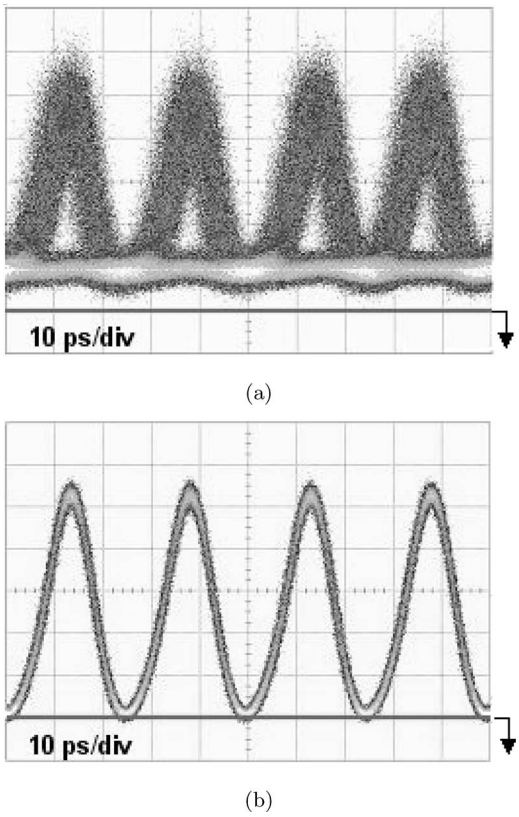

Fig. 12. (a) Eye diagram of the incoming signal with OSNR of 21 dB/0.1 nm. (b) Temporal traces of the recovered clock from the QD SP laser.

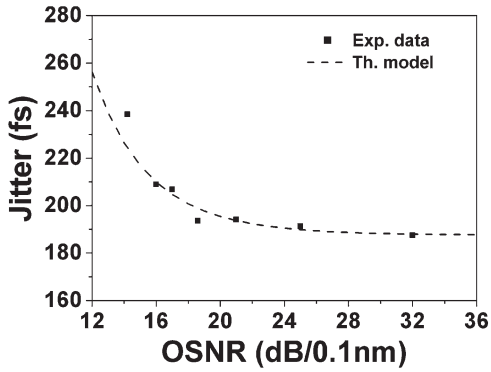

Fig. 13. Evolution of the timing jitter of the recovered clock from the QD SP laser as a function of the OSNR of the incoming signal.

The identical evolution of the experimental data and the interpolation curve clearly shows that the increase of timing jitter of the recovered clock is due to OSNR degradation of the incoming signal. Besides, we see that the QD SP laser exhibits a recovered clock with very low timing jitter (below 300 fs) even for degraded OSNR down to 14 dB/0.1 nm.

IV. Conclusion

In this paper, we have presented an exhaustive study of SP-laser-based all-optical-clock recovery at 40 GHz. Based on the SP-laser injection-locking theory, we have demonstrated the importance of the free running spectral linewidth of the SP laser on the phase-noise properties of the recovered clock, especially

on the cutoff frequency. From the phase-noise analysis of the recovered clock, we have expressed its timing jitter as a function of the contributions of the injected signal, the SP laser, and the OSNR of the injected signal. The experimental comparison between clock-recovery schemes using a bulk SP laser and a QD SP laser has demonstrated the impact of the spectral linewidth on the jitter-filtering efficiency. Moreover, the impact of the OSNR degradation of the injected signal has been demonstrated experimentally for OSNR lower than 30 dB/0.1 nm. Finally, we have also demonstrated the high potential of QD SP-laser-based approach for all-optical-clock recovery, with high extinction ratio and low timing jitter down to 14 dB/0.1 nm OSNR of the incoming signal.

APPENDIX
PHASE-NOISE PSD OF THE INCOMING SIGNAL WITH A GIVEN OSNR

We consider an optical-clock signal generated by an external modulator that can be expressed by the beating of three optical modes $\{-1, 0, +1\}$ with equal mode spacings of $f_{\rm in}$. Neglecting the harmonic at $2f_{\rm in}$ for the sake of simplicity, the optical power of the injected clock is expressed as follows:

$$P(t) = P_{\rm opt} + P_{\rm ck}\cos(2\pi f_{\rm in}t + \phi_{\rm ck}) \tag{18}$$

where $P_{\rm opt}$ is the average optical power equal to $\sum_{k=-1}^{1} P_k$, and the amplitude of the clock component $P_{\rm ck}$ is defined by

$$P_{\rm ck} = mP_{\rm opt} \tag{19}$$

where m is the modulation depth. The beating between these optical modes and the ASE noise generates intensity noise at the clock frequency $f_{\rm in}$, and the total power of the injected clock component may be written as

$$\begin{aligned} &P_{\rm in}\cos(2\pi f_{\rm in}t + \phi_{\rm in}) \\ &\quad = P_{\rm ck}\cos(2\pi f_{\rm in}t + \phi_{\rm ck}) + n(t)\cos(2\pi f_{\rm in}t + \phi) \end{aligned} \tag{20}$$

where $n(t)$ and $\phi(t)$ account for the amplitude and the phase of both signal-ASE beat noise and ASE-ASE beat noise. Hence, the ASE noise induces both amplitude and phase fluctuations of the oscillating power of the injected optical-clock signal. Assuming that these fluctuations are small compared to $P_{\rm ck}$, the total phase of the injected clock may be written as

$$\phi_{\rm in} = \phi_{\rm ck} + j\frac{n(t)}{P_{\rm ck}}e^{-j(\phi-\phi_{\rm ck})}. \tag{21}$$

Taking into account the noncorrelation between the clock component and the ASE noise, the phase-noise PSD of the oscillating power of the injected optical clock may be expressed as follows:

$$S_{\phi_{\rm in}}(f) = S_{\phi_{\rm ck}}(f) + \frac{S_n(f)}{P_{\rm ck}^2} \tag{22}$$

where S_n denotes the PSD of intensity noise around the carrier frequency $f_{\rm in}$. From [21] and [22], one can write this intensity noise PSD for a small frequency range ($\pm$500 MHz) around the carrier frequency as follows:

$$S_n(f) = 2P_{\rm opt}N_{\rm SP} + N_{\rm SP}^2 B_0\left(1 - \frac{f_{\rm in}+f}{B_0}\right) \tag{23}$$

where $N_{\rm SP}$ is the PSD of ASE noise, and B_0 is the bandwidth of the filter placed in front of the SP laser. The ASE noise is considered as a white noise. Introducing this expression into (22) and using the following definition of the OSNR:

$$\text{OSNR} = \frac{P_{\rm opt}}{N_{\rm SP}B_0} \tag{24}$$

the phase-noise PSD of the injected optical clock can be easily expressed as a function of the OSNR

$$\begin{aligned} S_{\phi_{\rm in}}(f) = S_{\phi_{\rm ck}}(f) + \frac{1}{B_0 m^2} \\ \times \left[\frac{2}{\text{OSNR}} + \left(1 - \frac{f_{\rm in}+f}{B_0}\right)\left(\frac{1}{\text{OSNR}}\right)^2\right]. \end{aligned} \tag{25}$$

ACKNOWLEDGMENT

The work presented in this paper was conducted in the framework of the French RNRT project "ROTOR."

REFERENCES

[1] A. Jourdan, "The perspective of optical packet switching inIP dominant backbone and metropolitan networks," *IEEE Commun. Mag.*, vol. 39, no. 3, pp. 136–141, Mar. 2001.

[2] B. Lavigne, P. Guerber, P. Brindel, E. Balmefrezol, and B. Dagens, "Cascade of 100 optical 3R regenerators at 40 Gbit/s based on all-active Mach–Zehnder interferometer," in *Proc. ECOC*, 2001, pp. 290–291.

[3] B. Lavigne, P. Guerber, D. Chiaroni, C. Janz, A. Jourdan, B. Sartorius, C. Bornholdt, and M. Morlhe, "Test at 10Gbit/s of an optical 3R regenerator using an integrated all-optical clock recovery," in *Proc. ECOC*, 1999, vol. II, pp. 262–263.

[4] B. Sartorius, C. Bornholdt, O. Brox, H. J. Ehrke, D. Hoffmann, R. Ludwig, and M. Mohrle, "All-optical clock recovery module based on self-pulsating DFB laser," *Electron. Lett.*, vol. 34, no. 17, pp. 1664–1665, Aug. 1998.

[5] C. Bornholdt, B. Sartorius, S. Schelbase, M. Mohrle, and S. Bauer, "Self-pulsating DFB laser for all-optical clock recovery at 40 Gb/s," *Electron. Lett.*, vol. 36, no. 4, pp. 327–328, Feb. 2000.

[6] O. Brox, S. Bauer, M. Biletzke, H. Ding, J. Kreissl, H.-J. Wunsche, and B. Sartorius, "Self-pulsating DFB for 40 GHz clock-recovery: Impact of intensity fuctuations on jitter," presented at the Optical Fiber Commun. Conf. (OFC), Los Angeles, CA, 2004, Paper MF55.

[7] T. Ohno, K. Sato, T. Shimizu, T. Furuta, and H. Ito, "Recovery of 40 GHz optical clock from 160 Gb/s data using regeneratively modelocked semiconductor laser," *Electron. Lett.*, vol. 39, no. 5, pp. 453–455, Mar. 2003.

[8] W. Mao, Y. Li, M. Al-Mumin, and G. Li, "All-optical clock recovery from RZ-format data by using a two-section gain-coupled DFB laser," *J. Lightw. Technol.*, vol. 20, no. 9, pp. 1705–1714, Sep. 2002.

[9] Y. Li, C. Kim, G. Li, Y. Kaneko, R. L. Jungerman, and O. Buccafusca, "Wavelength and polarization insensitive all-optical clock recovery from 96-Gb/s data by using a two-section gain-coupled DFB laser," *IEEE Photon. Technol. Lett.*, vol. 15, no. 4, pp. 590–592, Apr. 2003.

[10] H. Bao, Y. J. Wen, and H. F. Liu, "Impact of saturable absorption on performance of optical clock recovery using a mode-locked multisection semiconductor laser," *IEEE J. Quantum Electron.*, vol. 40, no. 9, pp. 1177–1185, Sep. 2004.

[11] G.-H. Duan, C. Gosset, B. Lavigne, R. Brenot, B. Thedrez, J. Jacquet, and O. Leclerc, "40 GHz all-optical clock recovery using polarization insensitive distributed Bragg refector lasers," presented at the Conf. Lasers Electro-Optics (CLEO), Baltimore, MD, 2003, Paper CThQ5.

[12] G.-H. Duan and G. Pham, "Injection locking properties of self-pulsation in semiconductor lasers," *Proc. Inst. Electr. Eng.—Optoelectron.*, vol. 144, no. 4, pp. 228–233, Aug. 1997.
[13] R. Adler, "A study of locking phenomena in oscillators," *Proc. IEEE*, vol. 61, no. 10, pp. 1380–1385, Oct. 1973.
[14] G. P. Agrawal and N. K. Dutta, *Long Wavelength Semiconductor Lasers*. New York: Van Nostrand, 1986.
[15] G.-H. Duan and G. Pham, "A new model of self-pulsating semiconductor lasers," in *Proc. SPIE—Physics Simulation Optoelectronic Devices VI*, San Jose, CA, 1998, vol. 3283, pp. 497–507. Part 1.
[16] K. Sato, "Optical pulse generation using Fabry–Pérot lasers under continuous-wave operation," *IEEE J. Sel. Topics Quantum Electron.*, vol. 9, no. 5, pp. 1288–1293, Sep./Oct. 2003.
[17] F. Lelarge, B. Rousseau, B. Dagens, F. Poingt, F. Pommereau, and A. Accard, "Room temperature continuous-wave operation of buried ridge stripe lasers using InAs-InP (100) quantum dots as active core," *IEEE Photon. Technol. Lett.*, vol. 17, no. 7, pp. 1369–1371, Jul. 2005.
[18] J. Renaudier, G.-H. Duan, J.-G. Provost, H. Debregeas-Sillard, and P. Gallion, "Phase correlation between longitudinal modes in semiconductor self-pulsating DBR lasers," *IEEE Photon. Technol. Lett.*, vol. 17, no. 4, pp. 741–743, Apr. 2005.
[19] J. Renaudier, R. Brenot, B. Dagens, F. Lelarge, B. Rousseau, F. Poingt, O. Legouezigou, F. Pommereau, A. Accard, P. Gallion, and G.-H. Duan, "45 GHz self-pulsation with narrow linewidth in quantum dot Fabry-Pérot semiconductor lasers at 1.5 μm," *Electron. Lett.*, vol. 41, no. 18, pp. 1007–1008, Sep. 2005.
[20] J. Renaudier, B. Lavigne, F. Lelarge, M. Jourdran, B. Dagens, O. Legouezigou, P. Gallion, and G.-H. Duan, "Standard-compliant jitter transfer function of all-optical clock recovery at 40 GHz based on a quantum-dots self-pulsating semiconductor laser," *IEEE Photon. Technol. Lett.*, vol. 18, no. 11, pp. 1249–1251, Jun. 2006.
[21] N. A. Olsson, "Lightwave systems with optical amplifiers," *J. Lightw. Technol.*, vol. 7, no. 7, pp. 1071–1082, Jul. 1989.
[22] G.-H. Duan and E. Georgiev, "Non-white photodetection noise at the output of an optical amplifier: Theory and experiment," *IEEE J. Quantum Electron.*, vol. 37, no. 8, pp. 1008–1014, Aug. 2001.

Jeremie Renaudier was born in Laval, France, on October 27, 1978. He received the B.S. degree from the Ecole Nationale Supérieure des Télécommunications (ENST-Bretagne), Brest, France, and the M.S. degree in optical communications and networks from the University de Bretagne Occidentale, Brest, both in 2002. He received the Ph.D. degree from the Ecole Nationale Supérieure des Télécommunications (ENST), Paris, France, in 2006. His Ph.D. dissertation was focused on the functional mode-locked DBR lasers for telecommunications applications at 40 Gb/s and beyond.

Bruno Lavigne received the Ph.D. degree in solid-state physics from the University Joseph Fourier, Grenoble, France, in 1990, for works on semiconductor II–VI materials.

In 1991, he joined Alcatel Alsthom Recherche, Marcoussis, France, where he was involved in research activities in the field of high- and low-temperature superconductors applied to telecommunication applications. From 1997 to 2003, he worked on optical regeneration techniques based on semiconductor optical amplifiers and adapted to optical transmissions or optical packet switching. He has been involved in several Advanced Communications Technologies and Services (ACTS) European projects dealing with the feasibility demonstration of an optical packet switching system and of optical processing functions. Since 2001, he has been a member of the Alcatel Technical Academy (ALTA). Since 2004, he has been working on transparent and reconfigurable networks aiming in the introduction of optics/optical functions in the core networks.

Philippe Gallion (M'82–SM'93) received the Doctorat de Troisième Cycle from the University of Reims, Reims, France, in 1975 and the Doctorat d'Etat from the University of Montpellier, Montpellier, France, in 1986.

In 1978, he was enrolled at the Ecole Nationale Supérieure des Télécommunications (ENST), also called Télécom Paris, where he is currently Full Professor. He is carrying out research at the Laboratoire de Traitement et Communication de l'Information (LTCI) joint research laboratories between ENST and the Centre National de la Recherche Scientifique (CNRS), where he is in charge of research activities in the fields of communications, electronics, radio frequencies, and optoelectronics. He has made pioneering contributions on laser noise, injection locking, semiconductor laser modulation chirp and tuning, coherent systems and optical devices, digital optical communications systems, and networks. His present research topics include theory, design, modeling, and characterization of functional devices, advanced optical digital communication systems and networks, radio over fiber systems, and quantum cryptography systems. He is author or coauthor of more than 180 technical papers and communications, and he has served as Advisor for more than 40 Ph.D. degree dissertations.

Prof. Gallion is a member of the Optical Society of America. He is the Chairman of the IEEE Laser and Electro Optics Society (LEOS) French Chapter. He serves on the Editorial Board and Scientific Committee of several technical publications and as member of program or steering committee of international scientific meetings.

Guang-Hua Duan (S'88–M'90–SM'01) was born in Hubei Province, China, on January 23, 1964. He received the B.E. degree from Xidian University, Xi'an, China, in 1983 and the M.E. and Doctorate degrees, both from the Ecole Nationale Supérieure des Télécommunications (ENST), Paris, France, in 1987 and 1991, respectively, all in applied physics.

He was habilitated to direct research by the Université de Paris-Sud, Paris, France, in 1995. He is now the Leader of the team "advanced photonic components" within Alcatel Thales III–V Laboratory, Marcoussis, France, with research activities on photonic crystals, advanced semiconductor lasers, optical amplifiers, and functional optoelectronic subsystems for core and metro networks. He lectures in the fields of electromagnetism, optoelectronics, and laser physics at ENST and with the Ecole Supérieure d'Optique. Previously, he was a Postdoctoral Fellow supported by both Alcatel Alsthom Research and ENST from 1991 to 1992. He was an Assistant and then an Associate Professor at ENST from 1992 to 2000. He was with the University of Maryland, College Park, as a Visiting Associate Professor from 1998 to 1999. He joined Opto+, Alcatel Research and Innovation Center, Marcoussis, in October 2000. He is the author or coauthor of more than 150 research papers, eight patents, and is a contributor to book chapters.

Dr. Duan is a member of la Société Française d'Optique.